Convenient Synthesis, Properties and the Structure of Tetramethylammonium Tris(pyrimidine-2-thiolato)ferrate(II): an Iron Complex with Three Stable Four-membered *N,S*-Chelate Rings

STEVEN G. ROSENFIELD, PRADIP K. MASCHARAK*

Department of Chemistry, Thimann Laboratories, University of California, Santa Cruz, Calif. 95064, U.S.A.

and SATISH K. ARORA

Drug Dynamics Institute, College of Pharmacy, University of Texas, Austin, Tex. 78712, U.S.A.

(Received September 26, 1986)

Abstract

Reaction of iron(II) chloride with sodium pyrimidine-2-thiolate in ethanol or methanol followed by addition of R_4NBr affords $(R_4N)[Fe(SC_4H_3N_2)_3]$ (R = Me, Et) in high yields. $(Me_4N)[Fe(SC_4H_3N_2)_3]$ crystallizes in the triclinic space group $P\bar{1}$ with a = 7.163(2), b = 10.002(3), c = 15.456(3) Å, α = 103.23(1)°, β = 91.25(1)°, γ = 92.09(1)° and Z = 2. The structure was refined to R = 2.9% on the basis of 5663 unique data ($F_o^2 > 2.5\sigma(F_o^2)$). The octahedral geometry about iron is highly distorted due to the presence of three four-membered chelate rings with an exceptionally small bite angle of *ca.* 67°. Average Fe–N and Fe–S distances are 2.163 and 2.529 Å respectively. The complex is isolated as the *mer* isomer. Mössbauer studies in polycrystalline state together with UV–Vis and magnetic susceptibility measurement in acetonitrile solution demonstrate that the iron is in +2 oxidation state with a high-spin electronic configuration.

Introduction

Pyridine-2-thiol (Py2SH, **1**), pyrimidine-2-thiol (Pm2SH, **2**), and their derivatives possess antiviral and antibacterial properties [1]. For example, compound **3** shows activity towards *Candida albicans* and *Bacillus cereus* at 100 and 50 ppm respectively [2] while compound **4** is active against *Staphylococcus aureus*, *Staphylococcus typhi* and *Bacillus subtilis* at 10–20 ppm level [3]. Since iron is a micronutrient, the antimicrobial properties exhibited by these compounds are expected to be related to the chemistry of their iron complexes. These chelating agents can compete for iron in microbial growth media thus depriving the organisms of the essential element. The other possibility is that the iron complexes are toxic. Indeed the toxic action of 8-hydroxyquinoline has been shown to be not due to withdrawal of an essential element but due to formation of a toxic complex [4]. In order to establish a structure–reactivity relationship for these antimicrobial agents, we have recently initiated a research project where we attempt to isolate specific iron complex(es) of these aromatic chelators and structurally characterize by X-ray crystallography. We also determine the level of toxicity of the iron complexes on several bacterial and fungal growths. Our goal is to sort out specific structural types which exhibit toxicity towards certain microorganisms. Recently we have reported the synthesis, structure and spectral properties of tetraethylammonium tris(pyridine-2-thiolato)ferrate(II) [5]. The unique feature of the structure is the presence of three four-membered chelate rings with an exceptionally small 'bite' angle of *ca.* 66°. We describe in this paper the synthesis, structure and spectroscopic properties of tetramethylammonium tris(pyrimidine-2-thiolato)ferrate-(II) (**5**) with all three Pm2SH ligands in the bidentate 'thiolate' form. The three chelated rings in the present compound are also four-membered indicating the stability of four-membered chelate rings with S donor atom(s).*

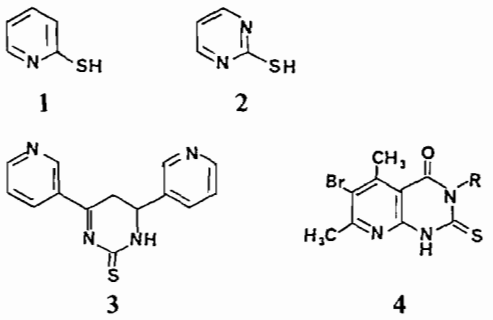

1 2 3 4

*Author to whom correspondence should be addressed.

*During the course of this research, the structure of the title compound was briefly reported by Latham *et al.* [30].

0020-1693/87/$3.50

© Elsevier Sequoia/Printed in Switzerland

Experimental

Preparation of Compounds

Pyrimidine-2-thiol was obtained from Aldrich Chemical Company and was used without further purification. $FeCl_2 \cdot 2H_2O$ was synthesized following literature procedure [6].

In the following two preparations, dry and degassed solvents were used and all manipulations were performed under a pure dinitrogen atmosphere.

$(Et_4N)[Fe(SC_4H_3N_2)_3]$

A solution of 0.82 g (5 mmol) of $FeCl_2 \cdot 2H_2O$ in 30 ml of ethanol was slowly added with continuous stirring to an ethanolic solution (80 ml) of 17.5 mmol of sodium pyrimidine-2-thiolate (from 0.40 g of sodium and 1.97 g of thiol). The initial pale yellow color gradually turned to deep red as the addition continued. A small amount of NaCl separated out as a white precipitate. Next, 1.15 g (5.5 mmol) of Et_4NBr in 30 ml of ethanol was added to it and the volume of the deep red reaction mixture was reduced to ~60 ml. It was then stored at −20 °C for 4 h. The red solid thus obtained was collected by filtration and was extracted into 50 ml of hot acetonitrile (~60 °C). The resulting dark red solution was kept at −20 °C for 48 h. The product came down as dark red needles which were collected by filtration, washed with 1:1 *v/v* acetonitrile/diethylether and dried *in vacuo*. 1.63 g (50%) of pure product was obtained. *Anal.* Calc. for $C_{20}H_{29}N_7FeS_3$: C, 46.22; H, 5.63; N, 18.88; Fe, 10.75. Found: C, 46.10; H, 5.65; N, 18.82; Fe, 10.82%.

$(Me_4N)[Fe(SC_4H_3N_2)_3]$ (5)

The addition of the ethanolic solution of $FeCl_2 \cdot 2H_2O$ to the solution of sodium pyrimidine-2-thiolate in ethanol was performed as described above using the same amounts and mole ratio of the reactants. 0.85 g (5.5 mmol) of Me_4NBr in 40 ml of methanol was added to the reaction mixture and the total volume was reduced to ~100 ml. It was then filtered and the dark red filtrate was stored at 0 °C. Large red blocks separated within 24 h which were collected by filtration, washed with 1:1 *v/v* acetonitrile/diethylether and dried *in vacuo*. A second crop of crystals was obtained from the filtrate on further volume reduction (~60 ml) and cooling (0 °C). Total yield: 1.18 g (51%). *Anal.* Calc. for $C_{16}H_{21}N_7FeS_3$: C, 41.45; H, 4.57; N, 21.16; Fe, 12.05. Found: C, 41.10; H, 4.69; N, 21.13; Fe, 11.97%.

In solid state, both the compounds are moderately sensitive to oxygen. The deep red solutions in acetonitrile, methanol or DMF, however, rapidly turn dark brown on exposure to oxygen.

Physical Measurements

All measurements were performed under strictly oxygen-free conditions. The solvents were dried over appropriate drying agents and freshly distilled under nitrogen prior to use. Electronic spectra were recorded either on a Cary Model 14 or Hitachi 100-80 spectrophotometer. Electrochemical measurements were performed with standard Princeton Applied Research instumentation using a Pt or glassy carbon working electrode. ^1H NMR spectra were recorded on a General Electric 300 MHz GN-300 instrument. Solution magnetic susceptibility was determined by the conventional NMR method using Me_4Si solution [7] and reference shift differences were measured to ±0.2 Hz using 30–40 mM solution of $(Et_4N)[Fe(SC_4H_3N_2)_3]$ in CD_3CN in coaxial tubes. Solvent susceptibility [8] and diamagnetic corrections [9] were taken from published data. Mössbauer spectra were obtained with a constant-acceleration spectrometer in the temperature range 300–4.2 K. Polycrystalline samples were dispersed in boron nitride powder. Spectra were measured in zero applied field and all ^{57}Fe isomer shifts are quoted *versus* Fe metal at room temperature. Microanalyses were performed by Galbraith Laboratories Inc., Tennessee. The % Fe was determined by EDTA titration using Variamine Blue as indicator [10].

Collection and Reduction of X-ray Data

Red blocks of **5** were obtained from slow cooling of methanol solution. A suitable crystal was sealed in a glass capillary. Diffraction experiments were performed on a Syntex $P2_1$ diffractometer with graphite-monochromatized Mo Kα radiation and a Syntex LT-1 inert-gas (N_2) low temperature delivery system. Data were obtained at 163 K. Data collection and structure refinement parameters are summarized in Table I. The orientation matrix and unit cell parameters were determined with 60 machine-centered reflections in the range $23.7° \leqslant 2\theta \leqslant 37.7°$. The intensities of check reflections were recorded after every 96 reflections to monitor crystal and instrument stability. Data were corrected for Lorentz and polarization effects, absorption and decay.

Solution and Refinement of the Structure

Non-hydrogen atomic scattering factors were taken from literature tabulations [11]. Atomic positions for the Fe and S atoms were obtained by direct methods program MULTAN and confirmed by Patterson method. The remaining non-hydrogen atoms were located from successive difference Fourier maps. The structure was refined by the least-squares method minimizing the function $\Sigma w(F_o - F_c)^2$ where $w = 1/\sigma^2(F_o)$. All non-hydrogen atoms were refined with anisotropic thermal parameters. Hydrogen atoms were located from a difference Fourier map, included in the model but not refined.

TABLE I. Summary of Crystal Data Intensity Collection and Structure Refinement Parameters for $(Me_4N)[Fe(SC_4H_3N_2)_3]$ (5)

Formula (molecular weight)	$C_{16}H_{21}N_7FeS_3$ (463.44)
a (Å)	7.163(2)
b (Å)	10.002(3)
c (Å)	15.456(3)
α (°)	103.23(1)
β	91.25(1)
γ	92.09(1)
Crystal system	triclinic
V (Å^3)	1076.7
Z	2
D_{calc} (g/cm^3)	1.429
D_{obs} (g/cm^3)	1.418[a]
Space group	$P\bar{1}$
Crystal dimensions (mm)	0.23 × 0.42 × 0.51
Radiation	Mo Kα (λ = 0.71069 Å)
Absorption coefficient μ (cm^{-1})	10.07
Transmission factors	Max = 0.804, Min = 0.622
Scan speed (°/min)	4–6
2θ limits (°)	$4.0 < 2\theta < 60.0$
Scan range (°)	(ω) symmetrically over 1.0 about $K\alpha_{1,2}$ maximum
Background/scan time ratio	1.0
Data collected	6487 ($\pm h, \pm k, +l$)
Unique data ($F_o^2 > 2.5\sigma(F_o^2)$)	5663
No. variables	244
Goodness of fit	0.048
R[b] (%)	2.9
R_w[c] (%)	3.1
Temperature (K)	163

[a]Determined by the neutral buoyancy technique in $ZnCl_2/H_2O$ system. [b]$R = \Sigma||F_o| - |F_c||/\Sigma|F_o|$. [c]$R_w = [\Sigma w(|F_o| - |F_c|)^2/\Sigma w|F_o|^2]^{1/2}$; $w = 1/\sigma^2(|F_o|)$.

Unique data used in the refinement and final R factors are given in Table I. Atomic positional parameters are listed in Table II. Selected bond distances and angles are presented in Table III. See also 'Supplementary Material'.

Results and Discussion

Tetraalkylammonium salts of tris(pyrimidine-2-thiolato)ferrate(II), $[Fe(S2Pm)_3]^-$ are isolated in high yields from the reaction in ethanol of 3.5 equivalent of preformed thiolate NaS2Pm with iron(II) chloride. As in the previously reported pyridine-2-thiolate complex $(Et_4N)[Fe(S2Py)_3]$ [5], all the three pyrimidine-2-thiolate ligands in $[Fe(S2Pm)_3]^-$ form four-membered chelate rings. Similar chelates with 2-hydroxypyridine or 2-hydroxypyrimidine are not known. Clearly chelation through sulfur enables stable four-membered rings in the thiolate complexes.

TABLE II. Positional Paramaters (10^4) for $(Me_4N)[Fe(SC_4H_3N_2)_3]$ (5)

Atom	x	y	z
Fe*	22018(3)	92200(2)	74791(2)
S(1)*	28712(7)	74384(5)	60872(3)
S(2)*	04896(6)	78618(5)	84397(3)
S(3)*	43410(6)	111266(5)	71999(3)
N(1)	0137(2)	9093(1)	6421(1)
N(2)	0105(2)	7710(2)	4938(1)
N(3)	3937(2)	8781(1)	8523(1)
N(4)	3154(2)	7548(2)	9629(1)
N(5)	1481(2)	11260(1)	8212(1)
N(6)	2922(2)	13440(2)	8164(1)
N(7)	6802(2)	4906(1)	6733(1)
C(1)	0852(2)	8124(2)	5763(1)
C(2)	−1453(3)	8326(2)	4780(2)
C(3)	−2291(3)	9298(3)	5403(2)
C(4)	−1430(3)	9663(2)	6238(2)
C(5)	2722(2)	8063(2)	8927(1)
C(6)	4926(3)	7781(2)	9938(1)
C(7)	6254(3)	8504(2)	9575(1)
C(8)	5685(2)	8993(2)	8852(1)
C(9)	2801(2)	12059(2)	7921(1)
C(10)	1660(3)	14040(2)	8740(1)
C(11)	0290(3)	13308(2)	9078(1)
C(12)	0254(2)	11892(2)	8789(1)
C(13)	5241(3)	4096(2)	6169(1)
C(14)	6004(3)	5826(2)	7524(1)
C(15)	8085(3)	3953(2)	7036(2)
C(16)	7863(3)	5738(2)	6208(1)

[a]Parameters for those atoms with asterisk were multiplied by 10^5.

The coordination chemistry of pyrimidine- and 4,6-dimethylpyrimidine-2-thiol (4,6Me$_2$Pm2SH)) is quite extensive [12–20]. Like Py2SH, Pm2SH can coordinate in the 'thiolate' or the tautomeric 'thione' form. In complexes of the type $M(4,6Me_2Pm2SH)_2X_2$ (M = Zn, Cd, Hg; X = Cl, Br, I), appearance of infrared bands in the 3200–3050 cm^{-1} (ν(NH)) region indicates monodentate coordination of the ligand in the thione form [16]. This is supported by ^{13}C and ^1H NMR studies [19]. Structures of three methylmercury derivatives of mercaptopyrimidines are known [21, 22]. In each case, the Hg atom is bonded to the thione S atom. In addition, there is a second strong interaction with Hg N distances at 2.80–2.95 Å. In tetrakis(1-methylpyrimidine-2-thione)zinc(II) perchlorate, zinc is tetrahedrally coordinated by the N(3) atoms of the four ligands [15]. There is no Zn–S interaction in the cation. The corresponding Mn and Co derivatives are isomorphous with the Zn complex. On the basis of spectral data, the majority of mercaptopyrimidine complexes have been assigned N,S-chelation of the ligand through the nonprotonated ring N and the exocyclic thione S atom. The metal–nitrogen bonds

TABLE III. Observed Distances and Angles in $[Fe(SC_4H_3N_2)_3]^-$

Distances (Å)					
Fe–S(1)	2.527(1)	N(1)–C(1)	1.357(2)	N(5)–C(12)	1.335(2)
Fe–S(2)	2.537(1)	N(1)–C(4)	1.332(3)	N(6)–C(9)	1.345(2)
Fe–S(3)	2.523(1)	N(2)–C(1)	1.341(2)	N(6)–C(10)	1.341(3)
Fe–N(1)	2.159(2)	N(2)–C(2)	1.339(3)	C(2)–C(3)	1.368(3)
Fe–N(3)	2.149(2)	N(3)–C(5)	1.359(2)	C(3)–C(4)	1.382(3)
Fe–N(5)	2.182(1)	N(3)–C(8)	1.333(2)	C(6)–C(7)	1.379(3)
S(1)–C(1)	1.735(2)	N(4)–C(5)	1.339(3)	C(7)–C(8)	1.378(3)
S(2)–C(5)	1.738(2)	N(4)–C(6)	1.339(3)	C(10)–C(11)	1.384(3)
S(3)–C(9)	1.727(2)	N(5)–C(9)	1.365(2)	C(11)–C(12)	1.384(3)
Angles (°)					
S(1)–Fe–S(2)	104.0(1)	C(1)–N(1)–C(4)	117.7(2)		
S(1)–Fe–S(3)	97.5(1)	C(1)–N(2)–C(2)	115.4(4)		
S(2)–Fe–S(3)	154.9(2)	C(5)–N(3)–C(8)	117.6(2)		
S(1)–Fe–N(1)	66.7(1)	C(5)–N(4)–C(6)	115.6(2)		
S(1)–Fe–N(3)	106.3(1)	C(9)–N(5)–C(12)	117.7(2)		
S(1)–Fe–N(5)	154.1(2)	C(9)–N(6)–C(10)	116.3(2)		
S(2)–Fe–N(1)	100.3(1)	S(1)–C(1)–N(1)	113.5(2)		
S(2)–Fe–N(3)	66.6(1)	S(1)–C(1)–N(2)	121.8(2)		
S(2)–Fe–N(5)	97.1(2)	N(1)–C(1)–N(2)	124.7(2)		
S(3)–Fe–N(1)	100.1(2)	N(2)–C(2)–C(3)	124.1(2)		
S(3)–Fe–N(3)	95.1(2)	C(2)–C(3)–C(4)	116.7(2)		
S(3)–Fe–N(5)	66.5(1)	C(3)–C(4)–N(1)	121.3(2)		
N(1)–Fe–N(3)	164.0(2)	S(2)–C(5)–N(3)	113.2(2)		
N(1)–Fe–N(5)	95.2(2)	S(2)–C(5)–N(4)	122.0(2)		
N(3)–Fe–N(5)	95.7(2)	N(3)–C(5)–N(4)	124.8(2)		
Fe–S(1)–C(1)	78.5(1)	N(4)–C(6)–C(7)	123.7(2)		
Fe–S(2)–C(5)	78.3(1)	C(6)–C(7)–C(8)	116.7(2)		
Fe–S(3)–C(9)	79.3(2)	C(7)–C(8)–N(3)	121.6(2)		
Fe–N(1)–C(1)	101.3(2)	S(3)–C(9)–N(5)	113.5(2)		
Fe–N(1)–C(4)	141.0(2)	S(3)–C(9)–N(6)	122.2(2)		
Fe–N(3)–C(5)	101.9(2)	N(5)–C(9)–N(6)	124.2(2)		
Fe–N(3)–C(8)	140.5(2)	N(6)–C(10)–C(11)	123.2(2)		
Fe–N(5)–C(9)	100.7(2)	C(10)–C(11)–C(12)	116.7(2)		
Fe–N(5)–C(12)	141.6(2)	C(11)–C(12)–N(5)	121.7(2)		

in such complexes however, appear to be considerably stronger than the metal–sulfur bonds [16] *viz.* in $Co(Pm2SH)_2Cl_2$, the Co–S distance is unusually long (2.960(2) Å) [13]. In tris(4,6-dimethylpyrimidine-2-thiolato)cobalt(III), the anionic ligand is justifiably bidentate since the Co–S bond lengths are normal and fall in the range 2.252–2.269 Å [12]. The iron complexes $Fe(Pm2SH)_2X_2$ (X = Cl, Br) are reported to be pseudooctahedral with weak Fe–S interaction [13]. Contrary to this observation, the Fe–S distances in **5** are close to the known Fe(II)–S_{th} (th = thiolate) bond lengths (*vide infra*). $Pm2S^-$ is also found as a bridging ligand in several dimeric complexes [23].

Structure of $(Me_4N)[Fe(SC_4H_3N_2)_3]$ (5)

An ORTEP drawing of the anion is shown in Fig. 1. Structural features of the cation are unexceptional and are not considered. The geometry around iron in **5** is distorted octahedral. The pyrimidine-2-

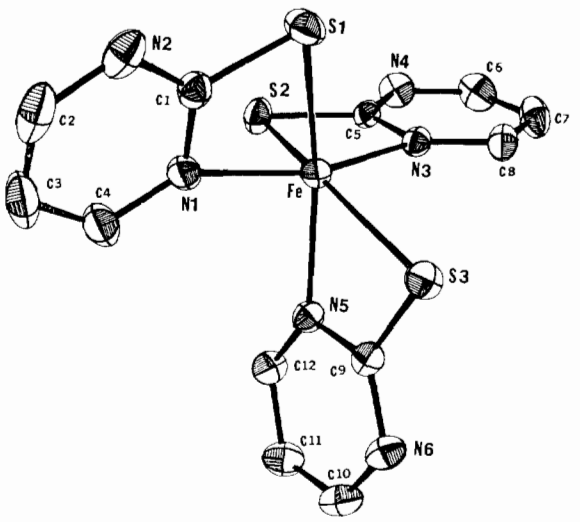

Fig. 1. Structure of $[Fe(SC_4H_3N_2)_3]^-$ in **5**, showing 50% probability ellipsoids and the atom labeling scheme.

thiolate ($Pm2S^-$) ligands coordinate through nitrogen and sulfur atoms such that two sulfur atoms are *trans* to each other while the third one is *trans* to a nitrogen atom. All the three chelate rings are four-membered with an N–M–S bite angle close to 67°. Thus the structure of $[Fe(S2Pm)_3]^-$ is very similar to that observed for $[Fe(S2Py)_3]^-$ [5].

The more important bond lengths and bond angles are listed in Table III. The Fe(II)–N distances in **5** fall in the narrow range 2.149–2.182 Å. Although no Fe(II)–N_{Pm} (Pm = pyrimidine) bond length is available for comparison, the Fe(II)–N_{Pm} distances in **5** are comparable to the Fe(II)–N_{Py} (Py = pyridine) distances (2.142–2.173 Å) in $[Fe(S2Py)_3]^-$ [5]. The Fe(II)–S_{th} bonds (2.523–2.537 Å) on the other hand, are shorter than the corresponding ones in $[Fe(S2Py)_3]^-$ (2.568–2.589) indicating stronger bonding interaction (*vide infra*). In tetrahedral thiolate complexes of iron, Fe(II)–S_{th} bond distances lie in the range 2.20–2.37 Å [24]. Strain in the four-membered chelate rings might be partly responsible for the lengthening of Fe(II)–S_{th} distances in **5**.

The angles about iron which show the greatest departure from ideal octahedral geometry are the N–Fe–S angles of *ca.* 67° (Table III). The two *trans* S and *trans* N atoms are also being drawn to each other; instead of 180°, the S2–Fe–S3 and N1–Fe–N3 angles are 154.9° and 164.0° respectively. In tris(4,6-dimethylpyrimidine-2-thiolato)cobalt(III), the N–Co–S angles are ~73° [12]. The small bite of the $Pm2S^-$ ligand brings about considerable strain in the ligand framework. For example, the Fe–N–C and N–C–S angles in **5** are distorted from 120°, expected for sp^2 hybridized atoms to ~101.0° and ~113.5° respectively. Similar deviations are also observed for Co–N–C (~99.5°) and N–C–S (~108.5°) angles in the cobalt complex.

In solution, Pm2SH exists almost exclusively in the thione form [25]. The presence of the thione form in solid state has been confirmed by X-ray crystallography [26]. The C–S bond lengths in thiocytosine and 2,4-dimercaptopyrimidine fall in the range 1.645–1.701 Å. The considerably short C–S bond lengths result from the contribution of the tautomeric thione form. In the tetrahedral zinc complex of 1-methylpyrimidine-2-thione where Zn–S interaction is negligible [15], mean C–S distance of 1.659 Å is observed. The C–S bonds in **5** however, are longer (mean = 1.733 Å) and are not strictly in the plane defined by the rings. These facts indicate that the ligands are coordinated as thiolates with very little contribution from the tautomeric thione form [5].

The spatial disposition of the donor centers around iron in **5** gives rise to the *mer* isomer. It is interesting to note that only the *fac* isomer of tris-(4,6-dimethylpyrimidine-2-thiolato)cobalt(III) has been isolated. The *cis* configuration of the S atoms has been rationalized on the ground that it allows maximum π back-bonding to S, since the orbitals of the three S atoms can overlap different metal orbitals [12]. In **5**, though the ligand is sterically less hindered, such stabilization factors are clearly overridden. Since $[Fe(S2Py)_3]^-$ [5] and $[Co(S2Py)_3]$ [27] are also isolated as the *mer* isomer, we believe that this geometrical isomer is energetically more favorable*. The steric crowding in the cobalt complex due to the presence of methyl groups on the ligands appears to be the major factor responsible for the successful isolation of the *fac* isomer with propeller-like shape. In the corresponding *mer* isomer, the methyl groups will be very close to each other thus making the arrangement energetically unfavorable.

Properties

Low temperature Mössbauer spectra in polycrystalline state and magnetic susceptibility measurements in solution at room temperature confirm the high-spin configuration of Fe(II) in $[Fe(S2Pm)_3]^-$. The Mössbauer spectrum of polycrystalline Et_4N^+ salt at 4.2 K, shown in Fig. 2 consists of a quadrupole doublet with isomer shift $\delta = 1.21 \pm 0.03$ mm/s and quadrupole splitting $\Delta E_Q = 3.96 \pm 0.05$ mm/s. These values are characteristic of high-spin ferrous ion in crystal field of low symmetry [28]. Similar δ and ΔE_Q values have been obtained for $(Et_4N)[Fe(S2Py)_3]$ [5]. The temperature dependence of ΔE_Q is however, quite different in these two cases. While $(Et_4N)[Fe(S2Py)_3]$ exhibits a strong dependence of ΔE_Q with temperature, only small reductions in ΔE_Q values of $(Et_4N)[Fe(S2Pm)_3]$ are observed with increasing temperature (Table IV). This behavior indicates the $Pm2S^-$ is a stronger ligand than $Py2S^-$ since variation of ΔE_Q with temperature arises from the population of the sixth electron on iron among levels split by the ligand field. Magnetic susceptibility measurement in acetonitrile solution at 296 K yields an effective magnetic moment of 5.38 BM for $(Et_4N)[Fe(S2Pm)_3]$ which also supports the high-spin ($S = 2$) configuration of Fe(II) in $[Fe(S2Pm)_3]^-$.

In acetontrile and DMF, $(R_4N)[Fe(S2Pm)_3]$ (R = Me, Et) exhibits a weak ($\epsilon \sim 10$, Table IV) double-humped absorption centered at 1270 and 900 nm. This absorption has been assigned to the only spin-allowed $^5T_{2g} \rightarrow {}^5E_g$ transition in octahedral high-spin Fe(II) complexes [5, 29]. The two maxima are 370 nm apart due to asymmetry in the crystal field and the inherent susceptibility of high-spin Fe(II) toward Jahn–Teller distortion. In the case

*$(Et_4N)[Ni(SC_5H_4N)_3]$ crystallizes in the monoclinic space group $P2_1/c$ with $a = 18.958(5)$, $b = 9.311(3)$, $c = 15.090(4)$ Å, $\beta = 104.91(2)°$ and $Z = 4$. The structure has been refined to $R = 4.68\%$ on the basis of 2636 unique ($F_o^2 > 3\sigma(F_o^2)$) data. The geometry around nickel is distorted octahedral. The complex is isolated as the *mer* isomer. Mean Ni–S = 2.528 Å, Ni–N = 2.052 Å, S–Ni–N angle = 67.53°.

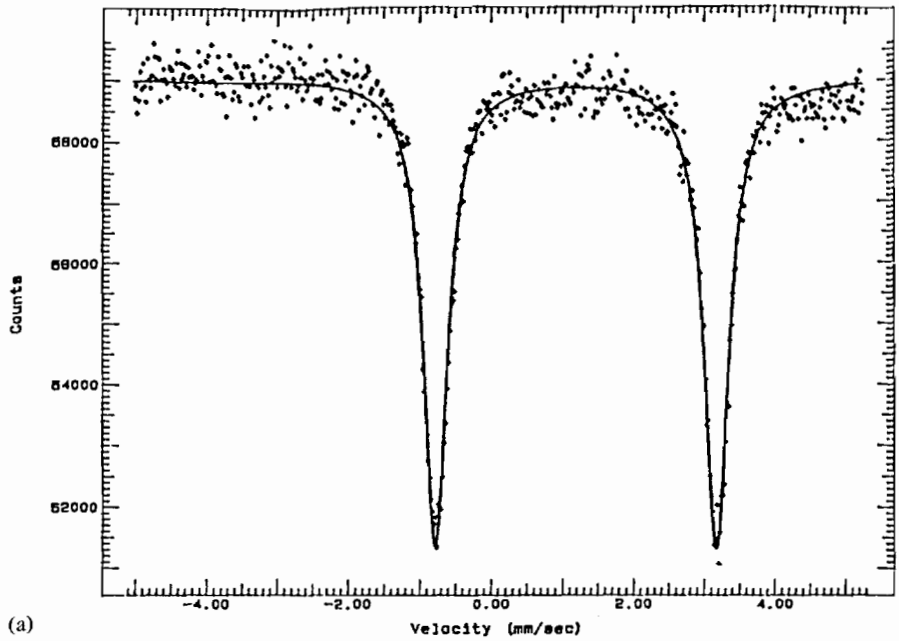

(a)

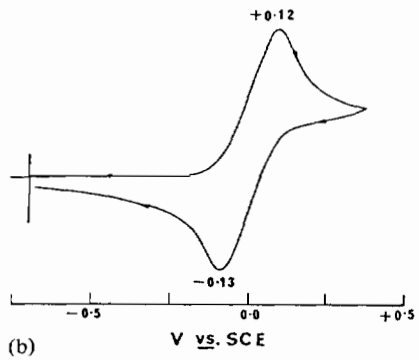

(b)

(c)

Fig. 2. (a) Mössbauer spectrum of polycrystalline $(Et_4N)[Fe(SC_4H_3N_2)_3]$ at 4.2 K. The solid line is a theoretical least-squares fit to the data assuming Lorentzian line shapes. (b) Cyclic voltammogram (50 mV/s) of $(Me_4N)[Fe(SC_4H_3N_2)_3]$ at Pt electrode in DMF solution. (c) ^1H NMR spectrum (300 MHz, ~298 K) of $(Et_4N)[Fe(SC_4H_3N_2)_3]$ in CD_3CN.

of $(Et_4N)(Fe(S2Py)_3]$, the bands appear at 1440 and 940 nm. The blue shift of the absorption maxima in $[Fe(S2Pm)_3]^-$ also confirms that $Pm2S^-$ is a stronger ligand than $Py2S^-$.

A clean one electron redox process is observed with $[Fe(S2Pm)_3]^-$. The voltammogram recorded in DMF at 50 mV/s is shown in Fig. 2. In DMF, the half wave potential is 70 mV more positive than

TABLE IV. Spectroscopic and Electrochemical Data for $(R_4N)[Fe(SC_4H_3N_2)_3]$

Solvent	$\lambda_{max}(\epsilon)$ (nm)	
Electronic spectrum		
MeCN	1270(8), 900(17), 490(1470), 330(5100)	
DMF	1270(8), 900(15), 500(1660), 340(5700)	
T (K)	δ[b,c] (mm/s)	ΔE_Q[c] (mm/s)
Mössbauer spectrum[a]		
230	1.10	3.61
150	1.15	3.89
77	1.18	3.97
4.2	1.21	3.96
Solvent	δ[d]	
	H_a	H_b
^1H NMR spectrum		
CD_3CN	50.83(1)	58.95(2)
$(CD_3)_2SO$	51.05(1)	60.32(2)
Solvent	$E_{1/2}$[f] (V)	
Half-wave potential[e]		
MeCN	-0.08 (ΔE_p = 110 mV)	
DMF	-0.01 (ΔE_p = 250 mV)	

[a]In boron nitride matrix. [b]Relative to Fe metal at room temperature. [c]Estimated uncertainties are ±0.03 mm/s in δ and ±0.05 mm/s in ΔE_Q. [d]ppm from TMS at 298 K, relative intensity of the peak in parentheses, see Fig. 2 for assignments of the peaks. [e]Cyclic voltammetry, Beckman Pt inlay electrode, 0.1 M tetrabutylammonium perchlorate as supporting electrolyte, 50 mV/s scan speed. [f]Values quoted *vs.* aqueous SCE.

that in acetonitrile (Table IV). The $E_{1/2}$ values clearly indicate that Pm2S$^-$ stabilizes Fe(II) more compared to Py2S$^-$ ($E_{1/2}$s for $[Fe(S2Py)_3]^-$ in DMF and acetonitrile are -0.21 and -0.27 V *versus* SCE respectively).

Two isotropically shifted resonances are located in the ^1H NMR spectra of $(R_4N)[Fe(S2Pm)_3]$ (R = Me, Et) which are assigned to the thiolato hydrogen atoms. The assignments of these two peaks, shown in Fig. 2, are based on the observed area ratio of 1:2.

Stability of four-membered N,S-chelate rings is well-documented in $[Fe(S2Py)_3]^-$ [5], $[Fe(S2Pm_3]^-$ (5), $[Co(S2Py)_3]$ [27] and $[Co(S2Pm4,6Me_2)_3]$ [12]. Recently, we have also synthesized (Et_4N)-$[Ni(S2Py)_3]$ in which three four-membered chelate rings are present. Studies on the toxicity properties of these metal complexes are in progress.

Supplementary Material

Thermal paramaters of cation and anion (Table S-I), bond distances and angles for the cation (Table S-II), positional parameters for hydrogens (Table S-III), unweighted least-square planes of the anion (Table S-IV), and the values of $10|F_o|$ and $10|F_c|$ (Table S-V) are available on request.

Acknowledgements

Support from a Faculty Research Committee Grant at University of California, Santa Cruz and NIH Grant GM32690 at University of Texas, Austin is gratefully acknowledged. We are also thankful to Drs. G. Papaefthymiou and R. Frankel of Francis Bitter National Magnet Laboratory, Massachusetts Institute of Technology, Cambridge Massachusetts for help in acquiring the Mössbauer spectra.

References

1 R. T. Coutts and A. F. Casy, in R. A. Abramovitch (ed.), 'Pyridine and its Derivatives', Suppl. Part IV, Wiley, New York, 1975, Chap. XVI, p. 453.
2 A. Attia and M. Michael, *Pharmazie, 37*, H.8 (1982).
3 C. G. Dave, P. R. Shah, V. B. Desai and S. Srinivasan, *Ind. J. Pharm. Sci., 44*, 83 (1982).
4 A. Albert, in 'Selective Toxicity', Methuen, London, 1968, p. 339.
5 S. G. Rosenfield, S. A. Swedberg, S. K. Arora and P. K. Mascharak, *Inorg. Chem., 25*, 2109 (1985).
6 K. H. Gayer and L. Woontner, *Inorg. Synth., 5*, 179 (1957).
7 D. F. Evans, *J. Chem. Soc.*, 2003 (1959); W. D. Phillips and M. Poe, *Methods Enzymol., 24*, 304 (1972).
8 W. Gerger, V. Mayer and V. Gutmann, *Monatsh. Chem.*, 417 (1977).
9 L. N. Mulay, in A. Weissberger and B. W. Rossiter (eds.), 'Physical Methods of Chemistry', Part IV, Wiley-Interscience, New York, 1972, Chap. VII.
10 A. Vogel, in 'Textbook of Quantitative Inorganic Analysis', Longman, New York, 1978, p. 322.
11 D. T. Cromer and J. T. Waber, 'International Tables for X-ray Crystallography', Vol. IV, Kynoch Press, Birmingham, U.K., 1974.
12 B. A. Cartwright, D. M. L. Goodgame, I. Jeeves, P. O. Langguth, Jr. and A. C. Skapski, *Inorg. Chim. Acta, 24*, L45 (1977); B. A. Cartwright, P. O. Langguth Jr. and A. C. Skapski, *Acta Crystallogr., Sect. B, 35*, 63 (1979).
13 J. Abbot, D. M. L. Goodgame, I. Jeeves, *J. Chem. Soc., Dalton Trans.*, 880 (1978).
14 R. Battistuzzi and G. Peyronel, *Transition Met. Chem., 3*, 354 (1978); D. M. L. Goodgame, G. A. Leach, A. C. Skapski and K. A. Woode, *Inorg. Chim. Acta, 31*, L375 (1978).
15 A. C. Skapski and K. A. Woode, *Acta Crystallogr., Sect. B, 35*. 59 (1979).
16 R. Battistuzzi and G. Peyronel, *Spectrochim. Acta, 36A*, 113 (1980).
17 D. M. L. Goodgame, I. Jeeves and G. A. Leach, *Inorg. Chim. Acta, 39*. 247 (1980).
18 R. Battistuzzi and G. Peyronel, *Can. J. Chem., 59*, 591 (1981).
19 R. Shunmugam and D. N. Sathyanarayana, *Ind. J. Chem., 22A*, 784 (1983).
20 R. Battistuzzi, *Polyhedron, 4*, 933 (1985).

21 C. Chieh, *Can. J. Chem.*, *56*, 560 (1978).
22 D. A. Stuart, L. R. Nassimbeni, A. T. Hutton and K. R. Koch, *Acta Crystallogr., Sect. B, 36*, 2227 (1980).
23 F. A. Cotton, R. H. Niswander and J. C. Sekutowski, *Inorg. Chem., 18*, 1149 (1979); F. A. Cotton and H. H. Ilsley, *Inorg. Chem., 20* 614 (1980); D. M. L. Goodgame, R. W. Rollins and A. C. Skapski, *Inorg. Chim. Acta, 83*, L11 (1984).
24 J. M. Berg and R. H. Holm, in 'Metal Ions in Biology', Vol. IV, 'Iron-Sulfur Proteins', Wiley, New York, 1982, Chap. I, and refs. therein.
25 A. Albert and G. B. Barlin, *J. Chem. Soc.*, 3129 (1962).
26 E. Shefter and H. G. Mautner, *J. Am. Chem. Soc., 89*, 1249 (1967); S. Furberg and L. H. Jensen, *Acta Crystallogr., Sect. B, 26*, 1260 (1970).
27 M. Kita, K. Yamanari and Y. Shimura, *Chem. Lett.*, 141 (1983).
28 N. N. Greenwood and T. C. Gibb, in 'Mössbauer Spectroscopy', Chapman and Hall, London, 1971, Chap. VI.
29 A. B. P. Lever, in 'Inorganic Electronic Spectroscopy', 2nd edn., Elsevier, Amsterdam, 1984, p. 458.
30 I. A. Latham, G. J. Leigh, C. J. Pickett, G. Huttner, I. Jibrill and J. Zubieta, *J. Chem. Soc., Dalton Trans.*, 1181 (1986).